

# 基于短光纤延时自外差的可见光单频激光线宽测量方法

王进<sup>1,2</sup>, 杨振管<sup>1,2</sup>, 李丰芮<sup>1,2</sup>, 单小琴<sup>1,2</sup>, 郑光金<sup>3</sup>, 韩正英<sup>3</sup>, 韩志刚<sup>1,2\*</sup>, 朱日宏<sup>1,2</sup>

<sup>1</sup>南京理工大学电子工程与光电技术学院, 江苏 南京 210094;

<sup>2</sup>南京理工大学先进固体激光工信部重点实验室, 江苏 南京 210094;

<sup>3</sup>中国电子科技集团公司第四十一研究所, 山东 青岛 266555

**摘要** 提出一种基于短光纤延时自外差法的可见光波段单频激光线宽测量方法, 利用短延时光纤减小可见光在石英光纤中的损耗并降低系统低频噪声, 通过频谱信号平滑方法极大地提高频谱数据的信噪比, 通过非线性最小二乘法拟合还原原始信号频谱, 并最终计算出可见光波段激光线宽。构建可见光波段的延时自外差测量系统, 搭建 127 m 和 500 m 延时光纤的可见光波段延时自外差测量装置, 测得 635 nm 单频外腔半导体激光器线宽为 29.4 kHz, 与两个相同型号激光器互拍的测量结果接近, 证明了基于短光纤延时自外差方法测量可见光单频激光器线宽的可行性。

**关键词** 测量; 线宽测量; 延时自外差法; 可见光激光器; 光学系统

中图分类号 O436

文献标志码 A

DOI: 10.3788/AOS231116

## 1 引言

可见光波段单频激光在波像差、长度量干涉测量以及频率标准中具有广泛应用<sup>[1-5]</sup>。在波像差干涉仪中<sup>[1-2]</sup>, 中心波长在 630 nm 附近单频激光器的相干性是空域干涉条纹对比度的保障, 决定了各类光学系统的波像差检测精度<sup>[6]</sup>。在长度量干涉仪中<sup>[3-5]</sup>, 激光器的频率特性直接影响长度量检测结果, 是光刻机位移台等精密位移装置的精度保障。在频率标准领域, 高频率稳定性的单频激光器是校准标定光谱仪、波长计等光谱装置的标准器具<sup>[7-8]</sup>。线宽是激光频率特性的重要指标, 它决定着激光器的相干性, 是保障激光应用的重要参数。精确测量线宽对于激光器的光学测量和频率标准等应用至关重要。

可见光波段单频激光的线宽参数测量通常采用光栅光谱仪<sup>[9-10]</sup>和法布里-珀罗标准具。光栅光谱仪仅能测得 GHz 量级的线宽<sup>[11-12]</sup>, 而法布里-珀罗标准具的极限测量精度也仅能到达 MHz 量级<sup>[13]</sup>。随着可见光波段单频激光器技术的进步, 该波段单频激光的线宽已经发展到 kHz 甚至 Hz 量级<sup>[14]</sup>, 显然这两种可见光常用的线宽测量手段已经无法满足现阶段可见光波段单频激光的线宽测量需求。利用两台独立的波长相近的激光器进行互拍频的双光束外差法能够实现 kHz 量级的

可见光单频激光器线宽测量<sup>[15]</sup>, 但该方法测量精度受限于激光器的频率稳定性, 测量误差较大。此外, 利用慢光干涉仪<sup>[16]</sup>可调控的相位差结合傅里叶变换分析也能够测量可见光波段激光线宽。延时自外差法<sup>[17-21]</sup>作为高精度的线宽测量方法, 在通信波段被广泛应用, 传统的延时自外差法利用长延时光纤来获取两束不相干的光, 延时光纤长度通常达到数十 km, 并通过移频器将拍频信号偏移零频以降低低频噪声影响。中国科学院苏州纳米技术和纳米仿生学研究所 Wu 等<sup>[22]</sup>利用 20 km 长的延时光纤测得中心波长为 1550 nm 的线宽为 5.06 kHz; 莫斯科国立大学 Fomiryakov 等<sup>[23]</sup>提出一种新的信号分析方法, 并利用 2 km 和 100 km 的光纤测得 kHz 量级的线宽。传统的长光纤延时自外差能够测量 kHz 量级的线宽, 但过长的光纤会使得低频噪声增大, 从而导致线宽测量结果出现误差<sup>[24]</sup>。由于传统的延时自外差法测量 kHz 量级的线宽就需要数十 km 的延时光纤, 近年来出现利用短光纤进行延时自外差的 kHz 量级线宽测量方法, 其基于相干包络分析的一种线宽测量理论: 重庆大学 Huang 等<sup>[25]</sup>和华中科技大学 Wang 等<sup>[26]</sup>通过判读干涉包络的峰值值差异, 将通信波段单频激光线宽检测精度提高到百 Hz 量级; 北京航空航天大学 He 等<sup>[27]</sup>和陕西科技大学 Xue 等<sup>[28]</sup>通过解调干涉包络信号分别测得通信波段的单频激光器线

收稿日期: 2023-06-12; 修回日期: 2023-07-11; 录用日期: 2023-08-30; 网络首发日期: 2023-09-10

基金项目: 国家自然科学基金(61875087)

通信作者: \*hannjust@163.com

宽为 2.5 kHz 和 151 Hz, 该方案在通信波段已经能够实现 kHz 甚至 Hz 量级的线宽测量。中国科学院国家授时中心高静等<sup>[29]</sup>还设计了一种基于短光纤循环外差法的线宽测量方法, 利用 2 km 延时光纤测得中心波长在 1050 nm 的激光器线宽为 944 Hz。但受限于可见光波段光纤的损耗和低信噪比导致的计算误差, 人们对于可见光波段单频激光的激光线宽测量技术鲜有研究。

本文提出一种基于短光纤延时自外差的可见光波段单频激光线宽测量方法, 搭建不同光纤长度的短光纤延时自外差系统, 通过小波变换及离群值消除平滑频谱中干涉包络线型, 并利用非线性最小二乘法拟合, 较为精确地还原干涉包络线型并测得可见光波段 635 nm 单频激光器线宽, 同时证明在不同长度的延时光纤下测量同一激光器线宽的一致性, 并与传统的两激光器互拍的双光束干涉自外差法进行对比, 实现可见光

波段单频激光的测量。

## 2 基本原理

图 1 为可见光波段短光纤延时自外差系统结构, 光纤耦合输出的单频激光器经偏振分束器 (PBS) 后分为两路光, 其中: 一路经光纤准直器输出为空间光经声光移频器 (AOM) 发生移频衍射, 经光阑选出正一级衍射光, 光频率发生改变; 另一路经延时光纤后由光纤准直器输出为空间光, 并与移频衍射光由合束晶体合束形成拍频信号, 最后经透镜聚焦在光电探测器 (PD) 光敏面上。光电探测器接收的拍频信号频谱由频谱仪采集。短光纤延时自外差拍频信号频谱如图 1 中红框所示, 红色虚线及标注是干涉包络旁瓣峰谷位置及其差的示意, 激光器线宽信息可以通过旁瓣峰谷值差  $\Delta S$  来求得。

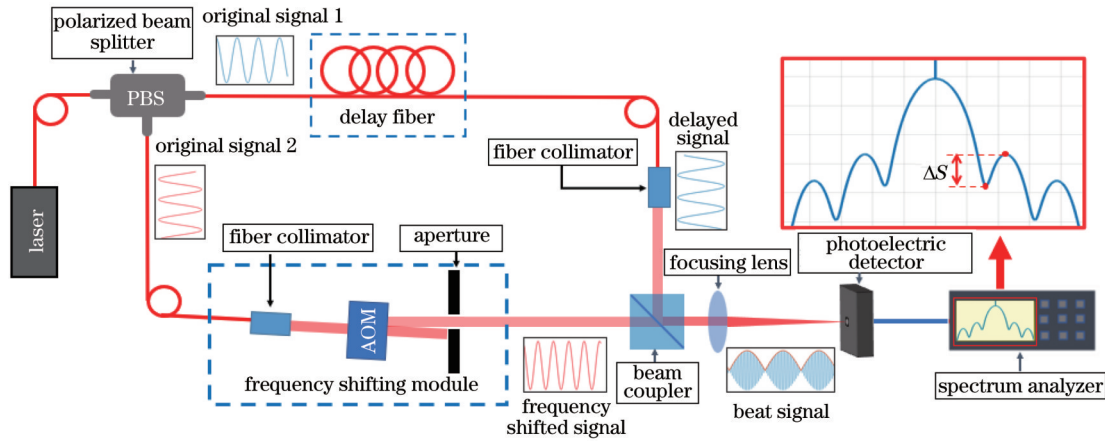


图 1 可见光波段短光纤延时自外差光路基本结构

Fig. 1 The basic structure of short fiber delay self-heterodyne system in visible light band

延时自外差拍频信号频谱<sup>[30]</sup>的数学表达式为

$$S(f) = S_1 \times S_2 + S_3, \quad (1)$$

式中:  $S_1$  为激光器的本征线宽项, 是标准的洛伦兹线型;  $S_2$  是延时光纤引入的调制项, 与延时量有关;  $S_3$  是拍频产生的脉冲项。它们的数学表达式<sup>[31]</sup>分别为

$$S_1 = \frac{P_0^2}{4\pi} \cdot \frac{\Delta f}{\Delta f^2 + (f - f_0)^2}, \quad (2)$$

$$S_2 = 1 - \exp(-2\pi\tau_d \Delta f) \left[ \cos[2\pi\tau_d(f - f_0)] + \Delta f \frac{\sin[2\pi\tau_d(f - f_0)]}{f - f_0} \right], \quad (3)$$

$$S_3 = \frac{\pi P_0^2}{2} \exp(-2\pi\tau_d \Delta f) \delta(f - f_0), \quad (4)$$

式中:  $P_0$  是激光器输出功率;  $f_0$  是声光移频器的移频量;  $\Delta f$  为激光线宽;  $f$  是拍频信号的频率;  $\delta(f - f_0)$  是在  $f_0$  频率处的一个脉冲信号;  $\tau_d$  是延时自外差系统的延时时间,  $\tau_d = nL/c$ ,  $n$  为光纤纤芯折射率,  $L$  为延时光纤长度。频谱中的  $S_1$  项是标准的洛伦兹线型, 为激光

器的本征线型, 它仅受激光线宽  $\Delta f$  的影响;  $S_2$  项为一个周期性函数, 其周期由延时量  $\tau_d$  决定, 其振幅则由激光线宽  $\Delta f$  和延时量  $\tau_d$  共同决定;  $S_3$  项是一个脉冲信号, 它为信号频谱引入一个在中心频差处的脉冲信号。

分析式 (1)~(4) 可知, 延时自外差拍频信号频谱的周期为

$$T_s = \frac{1}{\tau_d} = \frac{c}{nL}. \quad (5)$$

因此干涉包络旁瓣的峰谷值坐标与中心频率的差值可以表示为

$$\Delta f_m = \frac{(m+2)c}{2nL}, \quad (6)$$

式中:  $m$  为大于等于 0 的整数, 是峰谷值的序号。

图 2 为激光线宽为 20 kHz、延时光纤长度为 127 m 时的延时自外差信号频谱仿真及其峰谷值点对应的信号。

取峰谷值差  $\Delta S_{10}$ , 此时波谷序号  $m=0$ 、波峰序号  $m=1$ , 则有

$$\Delta S_{10} = 10\log S_1 - 10\log S_0 = 10\log \frac{S\left(f_0 + \frac{3c}{2nL}\right)}{S\left(f_0 + \frac{c}{nL}\right)} =$$

$$10\log \left\{ \frac{\frac{P_0^2}{4\pi} \times \frac{\Delta f}{\Delta f^2 + \left(\frac{3c}{2nL}\right)^2} \times \left[ 1 - \exp(-2\pi\tau_d \Delta f) \left[ \cos\left[2\pi\tau_d \left(\frac{3c}{2nL}\right)\right] + \Delta f \frac{\sin\left[2\pi\tau_d \left(\frac{3c}{2nL}\right)\right]}{\frac{3c}{2nL}} \right] \right]}{\frac{P_0^2}{4\pi} \times \frac{\Delta f}{\Delta f^2 + \left(\frac{c}{nL}\right)^2} \times \left[ 1 - \exp(-2\pi\tau_d \Delta f) \left[ \cos\left[2\pi\tau_d \left(\frac{c}{nL}\right)\right] + \Delta f \frac{\sin\left[2\pi\tau_d \left(\frac{c}{nL}\right)\right]}{\frac{c}{nL}} \right] \right]} \right\} =$$

$$10\log \left[ \frac{\Delta f^2 + \left(\frac{c}{nL}\right)^2}{\Delta f^2 + \left(\frac{3c}{2nL}\right)^2} \times \frac{1 - \exp(-2\pi\tau_d \Delta f) \cos(3\pi)}{1 - \exp(-2\pi\tau_d \Delta f) \cos(2\pi)} \right] = 10\log \left[ \frac{\Delta f^2 + \left(\frac{c}{nL}\right)^2}{\Delta f^2 + \left(\frac{3c}{2nL}\right)^2} \times \frac{1 + \exp(-2\pi\tau_d \Delta f)}{1 - \exp(-2\pi\tau_d \Delta f)} \right]. \quad (7)$$

式(7)描述了激光线宽  $\Delta f$  与第二峰谷值差  $\Delta S_{10}$  之间的关系。当延时光纤长度确定时,随着激光线宽增大,其对应的峰谷值差会减小,并最终趋向于 0。

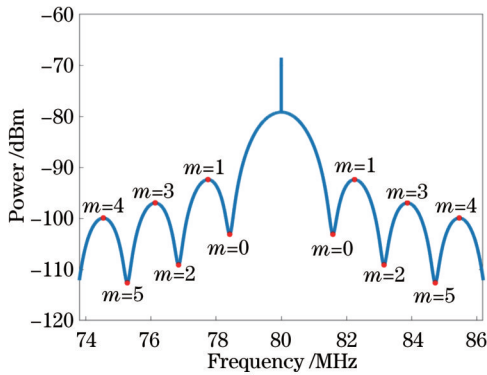


图 2 短光纤延时自外差拍频信号频谱峰谷值位置及其序号  
Fig. 2 Peak-valley position and serial number of short fiber delay self-heterodyne beat spectrum signal

在实际实验过程中,峰谷值差  $\Delta S_{10}$  可以从实验数据中采集判读,作为已知量代入式(7)中可以得到一个关于激光器线宽  $\Delta f$  的方程,通过求解该方程即可计算出被测激光器线宽。

### 3 原理仿真

图 3(a)是  $S, S_1, S_2, S_3$  的线型仿真,采用 dBm 为单位。仿真激光线宽为 70 kHz,延时光纤长度为 127 m。结合式(1)~(4)可以看出,信号频谱  $S$  可以看作是激光本征线型  $S_1$  受延时自外差系统引入的周期函数  $S_2$  调制后叠加一个脉冲函数得到的。图 3(b)是线宽为 30 kHz 的单频激光经不同长度的延时自外差系统后,拍频信号频谱的线型仿真。结合式(2)可以看出,随着

延时光纤长度的增加,拍频信号频谱的周期逐渐减小,当延时量趋向于无穷时,整体线型逐渐回归与激光本征线宽相关的洛伦兹线型。图 3(c)为延时光纤长度为 2 km 的延时自外差系统测量不同线宽激光器产生的拍频信号频谱线型仿真。结合式(4)可知,当延时光纤长度固定时,拍频信号频谱的周期不变,随着被测激光的线宽增加,拍频信号频谱线型逐渐趋于平缓,当延时量远大于激光的相干时间时,线型逐渐接近与激光本征线宽相关的洛伦兹线型。

图 4 为不同长度延时光纤的延时自外差拍频信号频谱的第二峰谷值差  $\Delta S_{10}$  随激光线宽  $\Delta f$  的变化曲线,从图中可以看出,同一长度延时光纤下,随着激光线宽增加,  $\Delta S_{10}$  逐渐减小。而激光线宽相同时,随着延时光纤长度增加,  $\Delta S_{10}$  逐渐减小。因此,短光纤延时自外差方案适用于窄线宽激光器的线宽参数测量,且理论上光纤长度越短其线宽分辨能力越好。

## 4 实验

### 4.1 实验设备

图 5 为可见光波段单频激光延时自外差线宽测量系统,开放摆设的光学器件可减少光纤器件的插入损耗,便于光路的调控。待测外腔半导体激光器(Newfocus, TLB7000, External-Cavity Diode Laser, 中心波长 635 nm)经光纤 PBS(铭创光电, S/N: 82136806 分束器)后分为两路正交偏振光,其中:一路经延时光纤(Nufem PM630-HP, 127 m, 工作波长 620~850 nm)后经光纤准直器(铭创光电, MCPMCO-630-100-2-00-P6-10-L-FA, 630 nm)输出,光在传播过程中偏振保持;另一路经光纤准直器(铭创光电, MCPMCO-630-100-2-00-P6-10-L-FA,

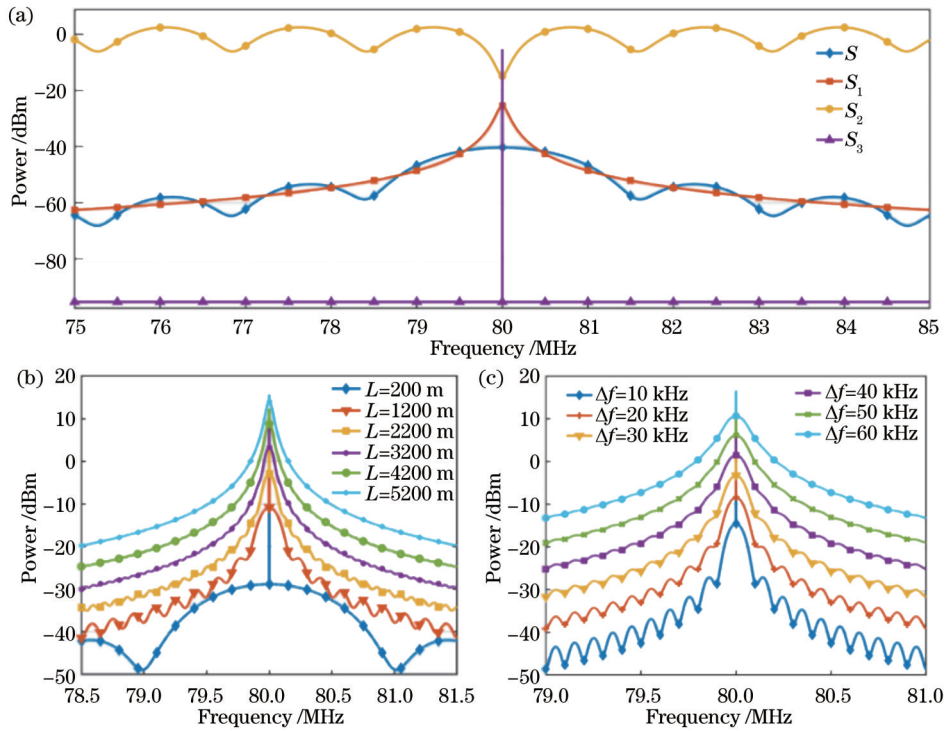


图 3 延时自外差信号频谱仿真。(a)线宽为 70 kHz、延时光纤长度为 127 m 时,延时自外差拍频信号  $S(f)$  及其组成部分的线型仿真; (b)线宽为 30 kHz 激光在不同长度延时光纤下拍频信号的频谱; (c)不同线宽的激光经延时光纤长度为 2 km 的延时自外差系统拍频信号的频谱

Fig. 3 The spectrum simulation of delay self-heterodyne beat signal. (a) The simulation of delay self-heterodyne beat signal  $S(f)$  and its components when the linewidth is 70 kHz and the delay fiber length is 127 m; (b) the spectrum of the beat signal of the 30 kHz laser under different length delay fibers; (c) the frequency spectrum of the beat signal of the laser with different linewidths passing through a delay self-heterodyne system with a delay fiber length of 2 km

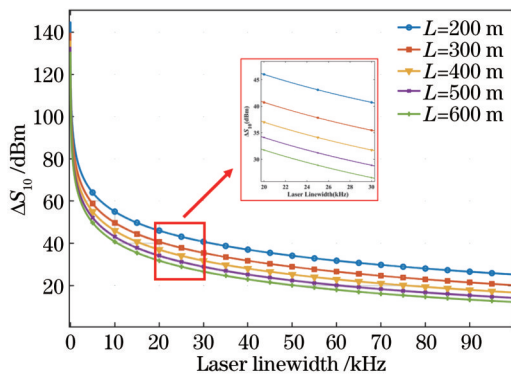


图 4 不同长度延时光纤下第二峰谷值  $\Delta S_{10}$  随线宽  $\Delta f$  的变化趋势

Fig. 4 The variation trend of the second peak-to-valley value  $\Delta S_{10}$  with the linewidth  $\Delta f$  under different length delay fibers

630 nm) 输出后经过声光调制器(中国电子科技集团第 29 研究所,SGT80-633-2TA, 80 MHz 移频),利用光阑选出正一级衍射光,之后经过半波片后将偏振调整至与另一路光相同,两束光经 BS 晶体合束后由透镜聚焦至光电探测器(迅秒光电,PD 300~1100 nm, 响应频率 1.5 GHz)接收拍频信号,最终频谱仪(RIGOL DSA1030)采集拍频信号频谱,设置频谱仪

扫描时间为 100 ms,在 100 ms 的时间尺度内,测试环境温度基本恒定且单次采集过程中没有震动发生。

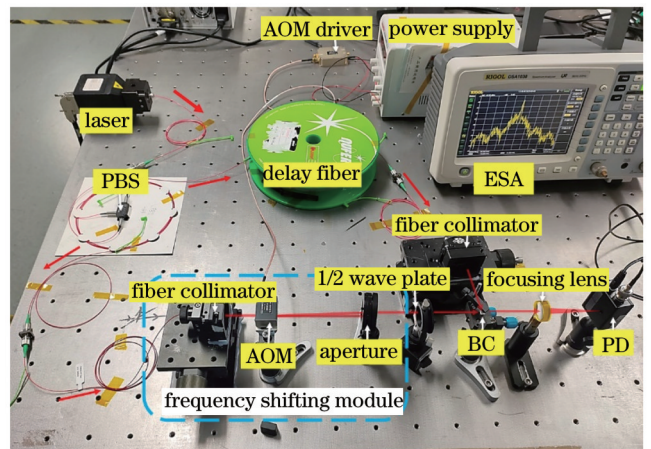


图 5 基于短光纤延时自外差的可见光波段单频激光线宽测量系统

Fig. 5 Single-frequency laser linewidth measurement system in visible light band based on short fiber delay self-heterodyne

图 6 为可见光波段传统的单频激光双光束外差线宽测量装置,该装置有两台独立的单频激光器,其中,被测激光器与短光纤延时自外差系统中激光器是同一

台(Newfocus, TLB7000, External-Cavity Diode Laser, 中心波长 635 nm), 且参考激光器与被测激光器型号相同。利用分束器(BS)晶体对两激光器的出射光进行合束, 形成两路拍频信号: 一路经透镜聚焦后入射到高速光电探测器(MenloSystems FPD310-FS-VIS, 响应频率 1500 MHz)上, 由频谱仪(Tektronix RSA5126B)分析拍频信号频谱; 另一路合束光经透镜耦合入光纤内, 光纤连接波长计(HighFiness WS7), 利用挡板遮挡激光来依次测量两激光器的输出波长。调节外腔激光器铌钛酸铅压电陶瓷(PZT)电压来改变激光器输出波长, 当两激光器的输出波长相近时可测得拍频信号频谱。

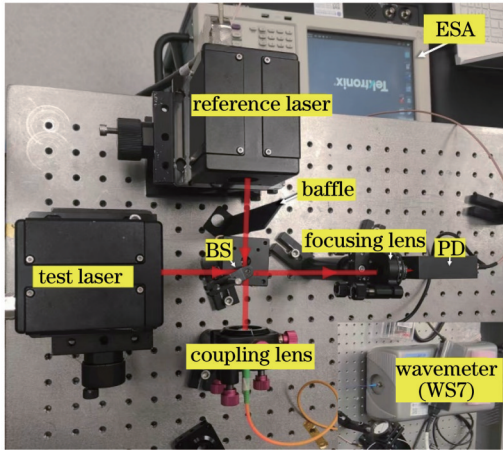


图 6 基于双光束外差法的可见光波段单频激光线宽测量装置  
Fig. 6 The single-frequency laser linewidth measurement device in visible light band based on dual-beam heterodyne method

## 4.2 实验结果

图 7 中蓝色曲线为频谱仪采集的外腔半导体激光器的延时自外差拍频信号频谱, 共有 601 个数据点。利用带有柯西先验的经验贝叶斯方法的小波变换对频谱中的数据点进行去噪, 最小限度为 9, 结果如图 7 中绿色 x 型标记曲线所示。进一步对小波消噪后的信号使用 MAD 法进行离群值的消除, 使信号进一步平滑, 最终信号如图 7 中红色菱形标记曲线所示。

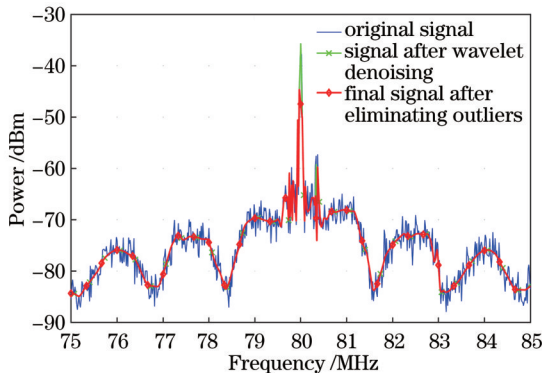


图 7 带噪声频谱信号的平滑过程  
Fig 7 Smoothing process of spectrum signal with noise

图 8 中蓝色曲线为频谱仪采集的外腔半导体激光器的延时自外差拍频信号频谱。延时自外差拍频信号中心频率在 80 MHz, 在其两侧有明显的干涉包络, 包络的第一谷值距离中心频率约为 1.68 MHz, 与 127 m 的延时光纤长度对应。由于光纤损耗较大, 产生的拍频信号功率较低, 因此拍频信号频谱信噪比较低。图 8 中绿色上三角标记曲线是对拍频信号频谱进行消噪平滑处理后的频谱, 可以明显看到频谱的信噪比有显著的提升。对平滑后的频谱信号的第一峰谷值进行判读, 第一谷值  $S_0$  为  $-83.21$  dBm, 第一峰值  $S_1$  为  $-73.28$  dBm, 峰谷值差  $\Delta S_{10}$  为  $9.03$  dBm。根据式 (7), 通过 Matlab 求得此时的线宽值为  $63.01$  kHz。利用解算的线宽值对比原始数据发现, 如果利用这个值来直接进行拟合的话会产生较大的误差, 因此只能将这个值作为初始值, 并利用平滑后的数据对式 (1) 进行非线性最小二乘法拟合, 结果如图 8 中红色菱形标记曲线所示, 拟合后得到的激光器线宽参数为  $29.71$  kHz。

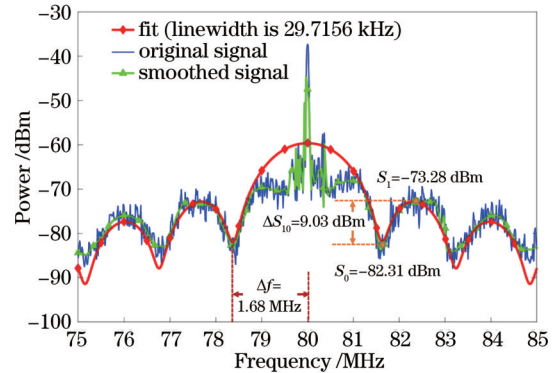


图 8 127 m 延时光纤下 635 nm 外腔半导体激光器延时自外差拍频信号频谱  
Fig. 8 Delayed self-heterodyne beat signal spectrum of 635 nm external-cavity diode laser with 127 m delay fiber

图 9 为 500 m 延时光纤 (YOFC, T0012005CC09, HP630, 工作波长 600~770 nm) 下同一外腔半导体激光器的延时自外差信号频谱。信号第一谷值距中心频率约为 0.4 MHz, 与 500 m 延时光纤对应。经过与之前信号平滑和拟合程序相同的步骤, 最终计算得到激光器线宽, 约为  $30.4506$  kHz。对比 127 m 和 500 m 延时光纤下激光器在延时自外差系统中得到的拍频信号频谱可以看出: 延时自外差信号频谱周期和峰谷值点都能与其延时光纤长度相对应, 符合理论公式; 且随着延时光纤长度增加, 损耗增大, 拍频信号信噪比降低。经过数据处理和拟合后, 不同长度延时光纤下的拍频信号频谱计算出来的线宽值几乎相同, 证明利用该方案测量激光器线宽对不同延时量的延时自外差系统具有一致性。

图 10 为传统的双光束外差法测量可见光波段激光线宽装置所获取的拍频信号的频谱信息。图 10 中

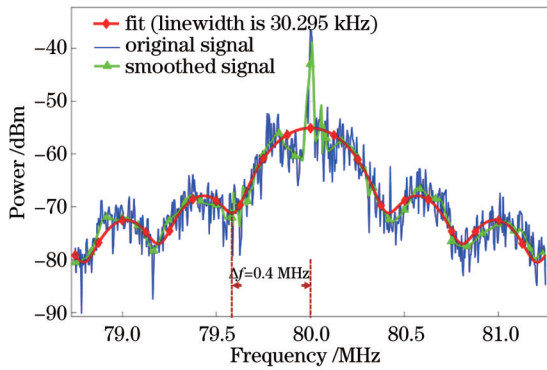


图 9 500 m 延时光纤下 635 nm 外腔半导体激光器延时自外差拍频信号频谱

Fig. 9 Delayed self-heterodyne beat signal spectrum of 635 nm external-cavity diode laser with 500 m delay fiber

蓝色曲线为频谱仪采集到的拍频信号频谱,红色菱形标记曲线为洛伦兹拟合后的线形。由于两激光器型号相同,其线宽大小也基本一致,因此单个激光器线宽约为拍频信号频谱 3 dB 带宽的一半<sup>[32]</sup>,根据拟合数据可知,激光器拍频信号频谱 3 dB 带宽为 104.43 kHz,故被测激光器的线宽大小约为 52.21 kHz。在测试过程中,利用 Highfinesse WS7 波长计测量该型号激光器的波长稳定性时,发现激光器波长会有一个约 0.001 pm/s 的波长漂移。频谱仪扫描时间为 100 ms,在 100 ms 内,两束激光波长并不稳定,因此在拍频的过程中会将两激光器波长漂移量计算到拍频信号频谱之中,导致线宽测量结果比实际要大。

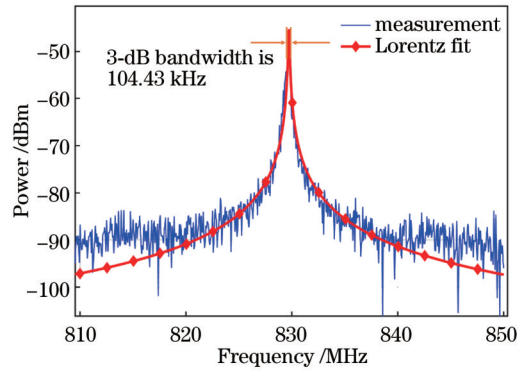


图 10 635 nm 外腔激光器双光束外差拍频信号频谱

Fig. 10 Frequency spectrum of two-beam heterodyne beat signal of 635 nm external-cavity diode laser

表 1 是短光纤延时自外差法和双光束外差法测量 635 nm 外腔半导体激光器线宽的多次测量结果。利用短光纤延时自外差法测量线宽时:127 m 延时光纤下测得线宽均值为 29.42 kHz,标准差为 1.36 kHz;500 m 延时光纤下 5 次线宽均值为 30.29 kHz,标准差为 2.24 kHz。双光束延时自外差法测得的 5 次线宽均值为 53.87 kHz,标准差为 4.51 kHz。分析数据可知:不同延时光纤长度的短光纤延时自外差法测量激光线宽具有重复性,且数据稳定性较好;双光束外差法在测量时由于激光波长稳定性不佳,因此测得的线宽值较大且测试稳定性较差,但其量级与短光纤延时自外差法测量结果基本一致,证明短光纤延时自外差法可以用来测量可见光波段单频激光的线宽值。

表 1 不同线宽测量方案多次测量结果

Table 1 Multiple measurement results of different linewidth measurement methods

unit:kHz

Serial number	Short fiber delay self-heterodyne method		Double-light-beam heterodyne method
	127 m delay fiber	500 m delay fiber	
1	29.71	30.45	52.21
2	28.91	30.38	58.69
3	31.58	35.55	47.09
4	27.96	31.54	54.46
5	28.91	30.29	56.90
Mean value	29.42	31.64	53.87
Standard deviation	1.36	2.24	4.51

## 5 讨 论

### 5.1 延时光纤长度选取范围

图 11 为不同线宽激光器的短光纤延时自外差频谱旁瓣第二峰谷值差  $\Delta S_{10}$  随延时光纤长度  $L$  变化的曲线。从图中可以看出,当激光器的线宽确定时,短光纤延时自外差信号频谱的第二峰谷值差  $\Delta S_{10}$  随光纤长度的增加而减小,在实际测量中, $\Delta S_{10}$  越大判读越准确,计算结果越准确,因此更短的光纤更容易获取准确的线宽值。而在可见光波段,最终形成的拍频信号会存

在一定的噪声,根据实验数据可知,在实际测量过程中频谱噪声峰谷(PV)值最高可达 5 dBm,因此对于百 kHz 的线宽, $\Delta S_{10}$  的值至少要大于 5 dBm,即延时光纤长度须小于 1 km。同时,考虑到可见光波段长光纤损耗较大,光强利用率低,拍频信号信噪比变差,因此要根据系统中移频路的参数来确定延时光纤的长度。采用的延时光纤损耗为 7 dB/km,声光移频器衍射效率约为 40%,并且考虑到光纤器件的插入损耗,延时光纤引入的损耗不应大于 4 dB,即光纤长度须小于 572 m。

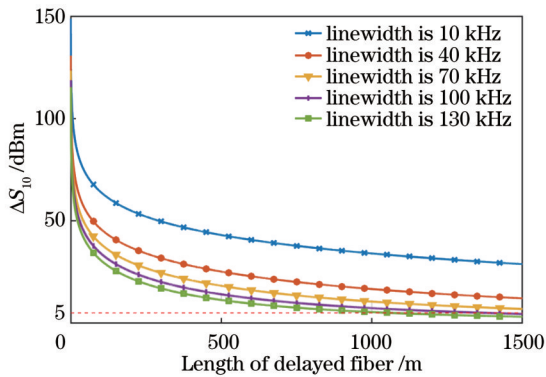


图 11 不同线宽激光器拍频信号频谱第二峰谷值  $\Delta S_{10}$  随光纤长度  $L$  的变化趋势

Fig.11 The variation trend of the second peak-to-valley value  $\Delta S_{10}$  of the beat frequency signal spectrum of different linewidth lasers with the fiber length  $L$

另一方面,由式(6)可知,随着延时光纤长度的减小,峰谷值距离拍频中心的频差  $\Delta f_m$  会逐渐增大,当延时光纤过短时,低频区的信号旁瓣会受到低频噪声影响,导致峰谷值判读和数据消噪拟合出现误差。一般来说,若要保证最小二乘法拟合的准确度,需要单侧信号旁瓣的两个信号峰来进行拟合,对应峰谷值序号  $m=5$ ,因此测量时需要保证低频峰值不受低频噪声影响。在本研究中,拍频信号频谱中心频率为 80 MHz,所用光电探测器引入的低频噪声分布如图 12 所示。通过判读可知,0~72 MHz 频率范围内存在较强低频噪声,若信号频谱分布在该范围内会受到较大的噪声影响,因此低频峰值所对应频率应大于 72 MHz,即  $\Delta f_5 < 8$  MHz,此时对应的光纤长度  $L > 88$  m。

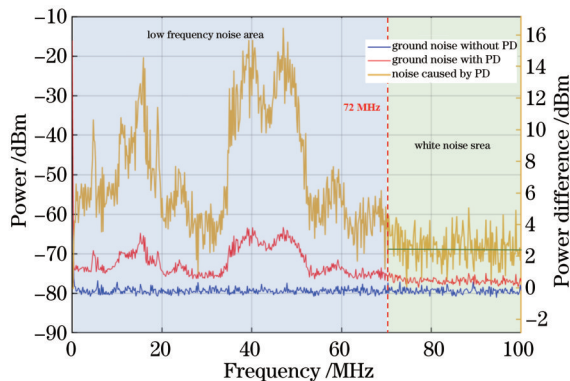


图 12 光电探测器的本底噪声

Fig. 12 Background noise of photodetectors

综上所述,所搭建的可见光波段短光纤延时自外差系统的延时光纤长度在 88~572 m 之间最佳,延时光纤长度的确定需综合考虑系统中各器件的参数和损耗。

## 5.2 1/f 相位噪声对短光纤延时自外差法的影响

利用干涉包络旁瓣峰谷值计算激光线宽基于式(7),本质上对于激光器线宽的定义是建立在激光线型

$S_1$  项是标准的洛伦兹线型之上的。但根据半导体激光器理论,受各类噪声的影响,激光器线型并不稳定,实际使用的激光器线型并不一定是标准的洛伦兹线型<sup>[33]</sup>。因此利用式(7)来计算激光器线宽仍会存在一定的误差,这也解释了为什么实验中利用式(1)作为拟合函数不能完全与实验数据相匹配。根据半导体激光器线型展宽理论,激光展宽后的线型存在一定的高斯线型成分,两者共同作用下可以将激光器线型抽象为 Voigt 函数<sup>[34]</sup>,利用该线型作为  $S_1$  对拍频信号频谱进行拟合可增加激光线宽测量的准确性。此外,通过判定 Voigt 函数中洛伦兹分量和高斯分量的成分还能够辅助分析半导体激光器的线型展宽理论,为激光器的纵模线型分析提供数据支持。

## 6 结 论

综上所述,提出一种基于短光纤延时自外差法的可见光单频激光器线宽测量方法,并搭建一套能够用于可见光波段激光线宽测量的短光纤延时自外差系统,短延时光纤避免可见光波段的高损耗,同时也降低因光纤延时引起的低频噪声。设计相应的拍频信号频谱平滑与拟合方法,提高可见光波段延时自外差频谱信噪比,还原拍频信号频谱,最终测得 635 nm 单频外腔半导体激光器线宽值,该方案在不同长度的延时光纤下具有一致性,并与传统双光束外差测量结果接近,实现了短光纤延时自外差法在可见光波段窄线宽激光器的线宽参数测量中的应用。

## 参 考 文 献

- [1] 袁群,季文,高志山.标准球面透镜的几何特性与误差分析[J].应用光学,2020,41(4):857-867.  
Yuan Q, Ji W, Gao Z S. Geometric characteristics and error analysis of standard spherical lens[J]. Journal of Applied Optics, 2020, 41(4): 857-867.
- [2] 胡乔伟,高志山,袁群,等.基于波像差判据的同步相移显微干涉检焦方法[J].应用光学,2021,42(4):703-708.  
Hu Q W, Gao Z S, Yuan Q, et al. Synchronous phase-shifting microscopic interference focal detection method based on wave aberration criteria[J]. Journal of Applied Optics, 2021, 42(4): 703-708.
- [3] 韩世泽,杨栋,胡晓宁,等.基于涡旋光与平面波干涉的微小位移测量[J].光学精密工程,2022,30(17):2058-2066.  
Han S Z, Yang D, Hu X N, et al. Micro-displacement measurement based on interference of vortex beams and plane wave[J]. Optics and Precision Engineering, 2022, 30(17): 2058-2066.
- [4] 胡晓宁,杨栋,杨忠明,等.共轭涡旋光干涉精密位移测量方法与系统[J].光学学报,2023,43(2):0212001.  
Hu X N, Yang D, Yang Z M, et al. Method and system for precision displacement measurement with interference of conjugated vortex beams[J]. Acta Optica Sinica, 2023, 43(2): 0212001.
- [5] 张金鹏,高芬,李兵.基于小孔点衍射的超精面形瞬态干涉测量技术[J].光子学报,2022,51(4):0412004.  
Zhang J P, Gao F, Li B. Transient interferometry of ultra precision surface based on small hole point diffraction[J]. Acta Photonica Sinica, 2022, 51(4): 0412004.

- [6] 朱日宏, 孙越, 沈华. 光学自由曲面形检测方法进展与展望[J]. 光学学报, 2021, 41(1): 0112001.  
Zhu R H, Sun Y, Shen H. Progress and prospect of optical freeform surface measurement[J]. Acta Optica Sinica, 2021, 41(1): 0112001.
- [7] 刘加庆, 刘磊, 刘雷, 等. 布里渊光谱仪的高精度波长标定方法研究[J]. 光学学报, 2020, 40(20): 2030001.  
Liu J Q, Liu L, Liu L, et al. Wavelength calibration of ultra-high resolution Brillouin spectrometer[J]. Acta Optica Sinica, 2020, 40(20): 2030001.
- [8] Sena A W, Hapiddin A, Syahadi M, et al. Optical wavelength meter calibration using iodine stabilized He-Ne laser by direct measurement method[J]. Procedia Engineering, 2017, 170: 363-368.
- [9] 盛灏, 华建文, 夏翔, 等. 近红外可见光傅里叶变换光谱仪的参考激光数字倍频方法研究[J]. 红外, 2014, 35(5): 29-33, 41.  
Sheng H, Hua J W, Xia X, et al. Design of digital frequency multiplier for near infrared and visible light Fourier transform spectrometer[J]. Infrared, 2014, 35(5): 29-33, 41.
- [10] 王宏博. 推扫式可见光/近红外成像光谱仪的在轨光谱定标与偏振校正技术研究[D]. 上海: 中国科学院上海技术物理研究所, 2016: 8-20.  
Wang H B. Research on in-orbit spectral calibration and polarization correction technology of visible/near-infrared pushbroom imaging spectrometer[D]. Shanghai: Shanghai Institute of Applied Physics, Chinese Academy of Sciences, 2016: 8-20.
- [11] 尹煜. 便携式拉曼光谱仪高精度 CCD 电路系统研究[D]. 杭州: 浙江大学, 2014: 3-13.  
Yin Y. Research on high precision CCD circuit system of portable Raman spectrometer[D]. Hangzhou: Zhejiang University, 2014: 3-13.
- [12] 许国春, 刘卫华. 一种高检测精度光谱仪: CN211477403U[P]. 2020-09-11.  
Xu G C, Liu W H. A high precision spectrometer: CN211477403U[P]. 2020-09-11.
- [13] Gwyn S, Watson S, Slight T, et al. Dynamic device characteristics and linewidth measurement of InGaN/GaN laser diodes[J]. IEEE Photonics Journal, 2020, 13(1): 1500510.
- [14] 柯旭, 邓乐武. 弱耦合互注入锁定半导体激光器的线宽研究[J]. 中国激光, 2022, 49(3): 0301001.  
Ke X, Deng L W. Linewidth of mutually injection-locked semiconductor lasers in weak coupling regime[J]. Chinese Journal of Lasers, 2022, 49(3): 0301001.
- [15] Blume G, Schiemangk M, Pohl J, et al. Narrow linewidth of 633-nm DBR ridge-waveguide lasers[J]. IEEE Photonics Technology Letters, 2013, 25(6): 550-552.
- [16] Shi Z M, Boyd R W, Camacho R M, et al. Slow-light Fourier transform interferometer[J]. Physical Review Letters, 2007, 99(24): 240801.
- [17] 汪滨波. 基于延时非零拍自外差法的窄线宽激光器线宽测量[J]. 新一代信息技术, 2022, 5(3): 50-52.  
Wang B B. Measurement of narrow linewidth laser based on delayed non-zero frequency self-heterodyne method[J]. New Generation of Information Technology, 2022, 5(3): 50-52.
- [18] Zhi Y Z, Feng L S, Lei M. Delay self-heterodyne measurement of narrow linewidth laser frequency drift characteristic[J]. Optik, 2014, 125(13): 3124-3126.
- [19] Zhang N, Rao W, Meng Z, et al. Linewidth study of the frequency-modulated laser based on the delayed self-heterodyne scheme[J]. Optics & Laser Technology, 2013, 45: 267-271.
- [20] Zhou Q, Qin J, Xie W L, et al. Dynamic frequency-noise spectrum measurement for a frequency-swept DFB laser with short-delayed self-heterodyne method[J]. Optics Express, 2015, 23(22): 29245-29257.
- [21] 刘霜, 李汉钊, 刘路, 等. 激光器频率噪声功率谱密度测试技术及在谐振式光纤陀螺中的应用[J]. 光学学报, 2021, 41(13): 1306010.  
Liu S, Li H Z, Liu L, et al. Laser frequency noise power spectral density measurement technology and its application to resonant optical fiber gyroscope[J]. Acta Optica Sinica, 2021, 41(13): 1306010.
- [22] Wu Y, Deng L H, Yang K Y, et al. Narrow linewidth external cavity laser capable of high repetition frequency tuning for FMCW LiDAR[J]. IEEE Photonics Technology Letters, 2022, 34(21): 1123-1126.
- [23] Fomiryakov E, Kharasov D, Nikitin S, et al. New approach to laser characterization using delayed self-heterodyne interferometry[J]. Journal of Lightwave Technology, 2021, 39(15): 5191-5196.
- [24] Mercer L B. 1/f frequency noise effects on self-heterodyne linewidth measurements[J]. Journal of Lightwave Technology, 1991, 9(4): 485-493.
- [25] Huang S H, Zhu T, Cao Z Z, et al. Laser linewidth measurement based on amplitude difference comparison of coherent envelope[J]. IEEE Photonics Technology Letters, 2016, 28(7): 759-762.
- [26] Wang Z H, Ke C J, Zhong Y B, et al. Ultra-narrow-linewidth measurement utilizing dual-parameter acquisition through a partially coherent light interference[J]. Optics Express, 2020, 28(6): 8484-8493.
- [27] He Y X, Hu S L, Liang S, et al. High-precision narrow laser linewidth measurement based on coherent envelope demodulation[J]. Optical Fiber Technology, 2019, 50: 200-205.
- [28] Xue M Y, Zhao J N. Laser linewidth measurement based on long and short delay fiber combination[J]. Optics Express, 2021, 29(17): 27118-27126.
- [29] 高静, 焦东东, 刘杰, 等. 基于短光纤循环自外差法的激光线宽测量[J]. 光学学报, 2021, 41(7): 0712002.  
Gao J, Jiao D D, Liu J, et al. Laser linewidth measurement based on recirculating self-heterodyne method with short fiber[J]. Acta Optica Sinica, 2021, 41(7): 0712002.
- [30] Zhao Z A, Bai Z X, et al. Narrow laser-linewidth measurement using short delay self-heterodyne interferometry[J]. Optics Express, 2022, 30(17): 30600-30610.
- [31] Richter L, Mandelberg H, Kruger M, et al. Linewidth determination from self-heterodyne measurements with subcoherence delay times[J]. IEEE Journal of Quantum Electronics, 1986, 22(11): 2070-2074.
- [32] 崔明斌, 黄俊刚, 杨修伦. 激光线宽测量方法的研究综述[J]. 激光与光电子学进展, 2021, 58(9): 0900005.  
Cui M B, Huang J G, Yang X L. Review on methods for laser linewidth measurement[J]. Laser & Optoelectronics Progress, 2021, 58(9): 0900005.
- [33] Di Domenico G, Schilt P, Thomann P. Simple approach to the relation between laser frequency noise and laser line shape[J]. Applied Optics, 2010, 49(25): 4801-4807.
- [34] Chen M, Meng Z, Wang J F, et al. Ultra-narrow linewidth measurement based on Voigt profile fitting[J]. Optics Express, 2015, 23(5): 6803-6808.



# Linewidth Measurement of Visible Single-Frequency Laser Based on Short-Fiber Delay Self-Heterodyne

Wang Jin<sup>1,2</sup>, Yang Zhenying<sup>1,2</sup>, Li Fengrui<sup>1,2</sup>, Shan Xiaoqin<sup>1,2</sup>, Zheng Guangjin<sup>3</sup>,  
Han Zhengying<sup>3</sup>, Han Zhigang<sup>1,2\*</sup>, Zhu Rihong<sup>1,2</sup>

<sup>1</sup>*School of Electronic and Optical Engineering, Nanjing University of Science & Technology, Nanjing 210094, Jiangsu, China;*

<sup>2</sup>*MIIT Key Laboratory of Advanced Solid Laser, Nanjing University of Science & Technology, Nanjing 210094, Jiangsu, China;*

<sup>3</sup>*The 41st Research Institute of China Electronics Technology Group Corporation, Qingdao 266555, Shandong, China*

## Abstract

**Objective** Visible single-frequency lasers have important applications in optical precision measurement and frequency standards. As an important parameter to determine laser coherence, linewidth guarantees the contrast of spatial interference fringes and directly determines the accuracy of the measurement system. In the visible light band, common measurement methods for laser linewidth are employing spectrometers and F-P cavities, but the measurement accuracy of these methods can only reach GHz and MHz levels, which cannot meet the current requirements of kHz or even Hz levels for linewidth measurement accuracy. As a new linewidth measurement method, the short-fiber delay self-heterodyne method can realize kHz linewidth measurement in communication bands, but the applications in visible light bands are rarely studied. Since the short-fiber delay self-heterodyne method can obtain high-precision linewidth without adopting too long optical fiber, it is a potential means to measure the laser linewidth in visible light bands.

**Methods** We propose a measurement method of visible single-frequency lasers based on the short-fiber self-heterodyne method, which introduces the short-fiber delay self-heterodyne method in the communication bands into the visible light bands and realizes linewidth measurement of high-precision lasers in the visible light bands. The principle of the proposed method is that the laser beams are split by the beam splitter (BS), one path is time-delayed by the delay fiber, and the other path's frequency is shifted by the acousto-optic modulator (AOM). The two laser beams are combined by a beam combiner (BC) to obtain a beat signal. Since the optical path difference introduced by the delay fiber is much smaller than the laser coherence length, an interference envelope will appear around the center frequency in the spectrum of the beat frequency signal, and the sidelobe of the envelope contains the laser linewidth information. We design a short-fiber delay self-heterodyne optical path as shown in Fig. 1 to interpret the sidelobes of the interference envelope and obtain the second peak-valley value  $\Delta S_{10}$  of the sidelobes. According to the spectrum expression of the beat frequency signal, we obtain the equation [equation (7)] about the laser linewidth, and the laser linewidth can be obtained by solving this equation. Due to the low signal-to-noise ratio (SNR) of the beat signal, we design a data smoothing method based on wavelet transform and outlier elimination. Meanwhile, we adopt the solution of equation (7) as the initial value, and utilize the nonlinear least squares method to fit the smoothed curve to obtain the accurate linewidth. Additionally, we set up a visible single-frequency laser linewidth test system as shown in Fig. 5, employ different lengths of delay fibers to test the same laser, and compare the test results with the traditional double-beam heterodyne method. Finally, the linewidth of an external cavity semiconductor laser with a center wavelength of 635 nm is measured.

**Results and Discussions** We put forward a linewidth measurement method of visible single-frequency lasers based on the short-fiber delay self-heterodyne method, and build a short-fiber delay self-heterodyne system that can be adopted for the laser linewidth measurement in the visible light bands. An external cavity diode laser with a center wavelength of 635 nm under the 127 m long delay fiber is measured, and the measured beat signal spectrum is shown in Fig. 7, where the blue curve is the original data, the green curve is the smoothed curve, and the red curve is the curve after fitting the smooth data. Several laser measurements show that the average laser linewidth is about 29.42 kHz with a standard deviation of 1.36 kHz. We employ the 500 m system delay fiber and the measured spectrum data are shown in Fig. 8. After measuring the laser linewidth several times by the 500 m fiber, the measured average laser linewidth is about 31.46 kHz, with a standard deviation of 2.24 kHz. Additionally, we leverage a laser of the same type as the laser under test to beat each other. The experimental device and the measured beat signal spectrum are shown in Fig. 6 and Fig. 9 respectively, and the average laser linewidth calculated by multiple measurements is 53.87 kHz, with the standard deviation is 4.51 kHz.

Considering that the laser frequency instability will affect the beat frequency signal during the test, the measurement results of this measurement method are close to those of the short-fiber delay self-heterodyne method.

Employing equation (7) to calculate the laser linewidth is based on the fact that the  $S_1$  item of the laser line shape is above the standard Lorentz line shape. However, according to the semiconductor laser theory, the laser line shape is unstable due to the influence of various noises and is not the standard Lorentz line shape. Therefore, adopting equation (7) to calculate the laser linewidth will cause some errors, which also explains the reason why utilizing equation (1) as a fitting function in the experiment cannot completely match the experimental data. According to the line-shape broadening theory of semiconductor lasers, there will be a certain Gaussian line-shape component in the line-shape after the laser broadening, and the laser line-shape can be abstracted into a Voigt function under the joint action of the two. Additionally, this line shape can be employed as  $S_1$  to fit beat frequency signal spectrum for increasing the accuracy of laser linewidth measurements.

**Conclusions** To sum up, we build a set of short-fiber delay self-heterodyne systems that can be adopted for laser linewidth measurement in the visible light bands. The short-delay fiber avoids high loss in the visible light bands and also reduces the low-frequency noise caused by fiber delay. Meanwhile, we design the corresponding smoothing and fitting methods of the beat-frequency signal spectrum to increase the low signal-to-noise ratio of the delay self-heterodyne spectrum in the visible light bands. Finally, the linewidth of a 635 nm single-frequency external cavity semiconductor laser is measured. This scheme has consistency under different lengths of delay fibers and is close to the traditional double-beam heterodyne measurement results. We prove that the short-fiber delay self-heterodyne method in linewidth parameter measurement of narrow linewidth lasers in the visible light bands is feasible.

**Key words** measurement; linewidth measurement; delay self-heterodyne method; visible laser; optical system